

# It's Not Easy Being Green: Kinetic Calculations Simulating the Emission Spectra of STEVE's Picket Fence

L. Claire Gasque<sup>1</sup>, Reza Janalizadeh<sup>2</sup>, Brian J. Harding<sup>1</sup>, D. Megan Gillies<sup>3</sup>

<sup>1</sup>Space Sciences Lab, University of California, Berkeley; <sup>2</sup>The Pennsylvania State University; <sup>3</sup>University of Calgary



## Debating the Origin of STEVE's Picket Fence

STEVE (Strong Thermal Emission Velocity Enhancement), a subauroral optical phenomenon, features a narrow mauve arc and vibrant green streaks called the picket fence (Fig. 1) [1]. Early research suggested picket fence emissions arise from magnetospheric particle precipitation [2,3], but later analysis revealed spectral features that challenged this hypothesis, including the absence of 427.8 nm  $N_2^+ 1N$  emissions which are ubiquitous in aurora [4]. Recent studies propose that the picket fence is formed when electric fields parallel to Earth's magnetic field energize local electrons [5,6]. However, it remains to be shown that parallel fields can lead to emissions consistent with observed spectra.



Fig 1: STEVE and the picket fence [1]

We present new observations and modeling results to assess whether parallel electric fields can energize electrons in a manner consistent with observed picket fence emission spectra.

## Picket Fence Observations

The TREx spectrograph [7] observed the picket fence between 6:25 and 8:00 UT on 10 April 2018 (Fig. 2a). For our analysis, we used 45 spectra, all with elevation angles between 130° and 145° (e.g. Fig. 2b), where 0° is due North. Fig. 2c summarizes the picket fence observation geometry.

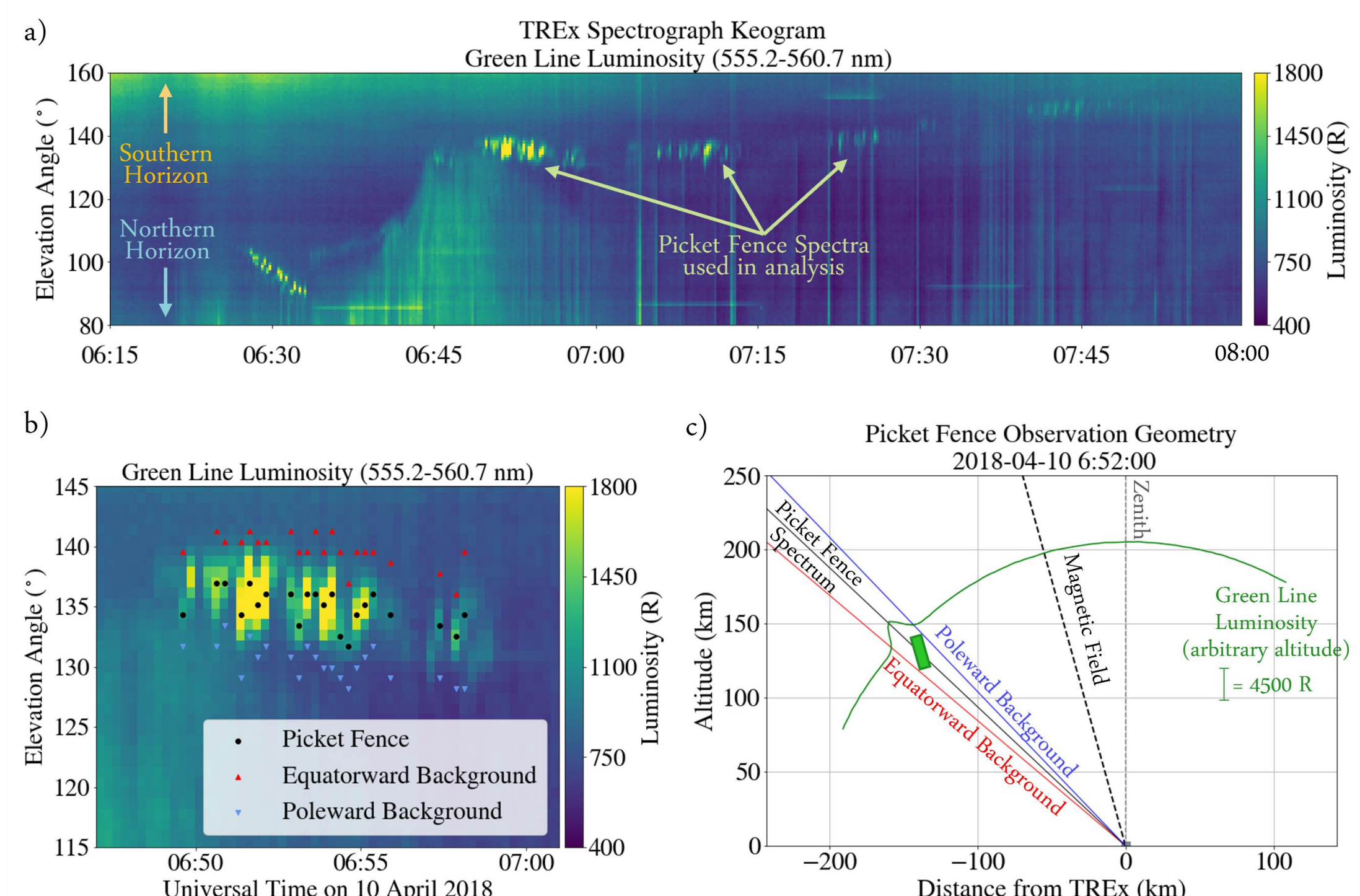
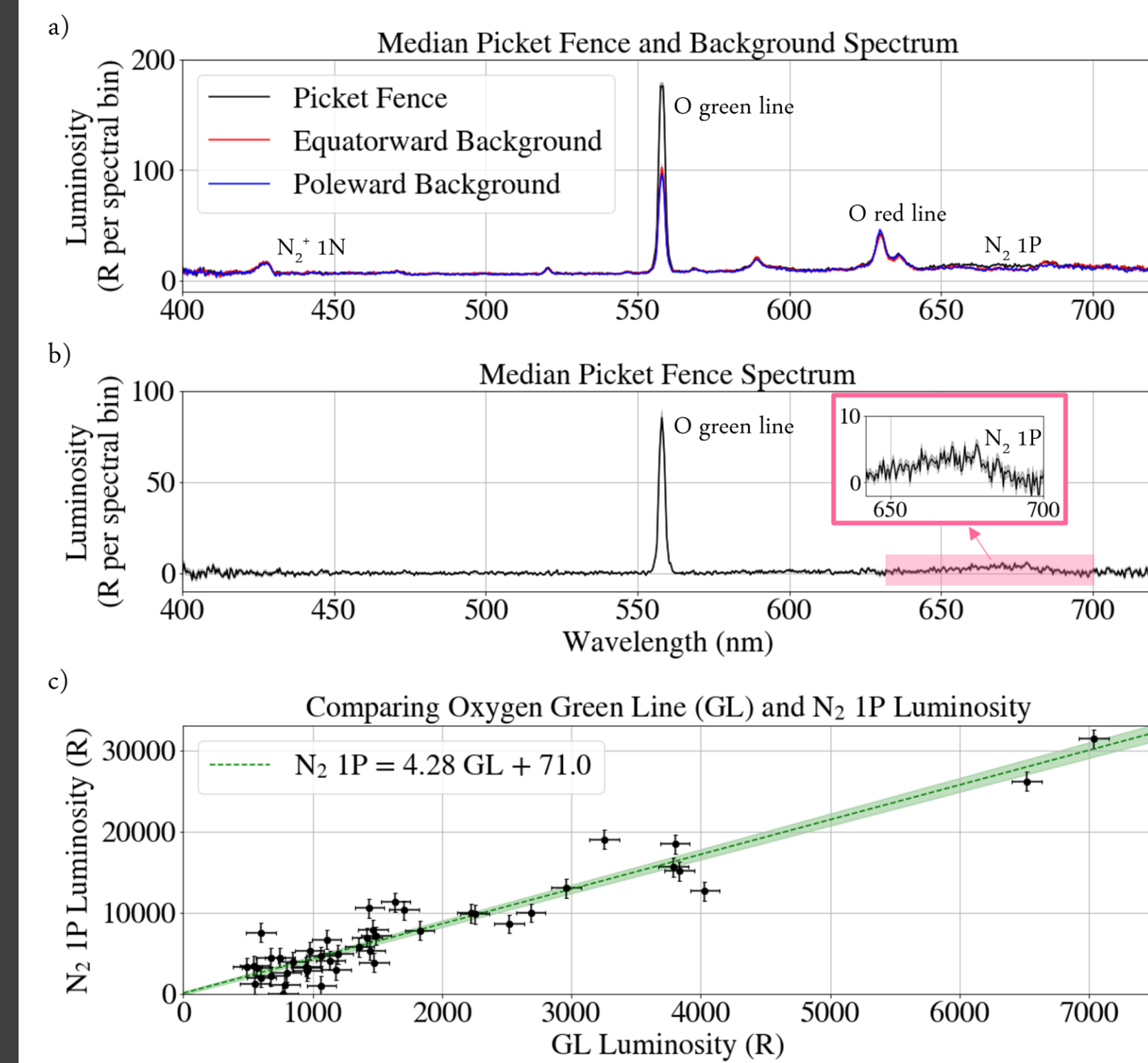


Fig 2: (a) Keogram of the oxygen green line (GL) 557.7 nm emissions observed by the TREx spectrograph, pointing out the events used in this study.

(b) Sample spectral extraction displaying the times and elevation angles of the picket fence and background spectra extracted from 6:49 to 7:00 UT. We extracted spectra using a Gaussian fit at each timestep, setting the background to be  $3\sigma$  away from the peak.

(c) Sketch depicting the picket fence observation geometry at 6:52 UT. Note that the 'sample picket' shown (green rectangle) is only a representation as the emission altitude is unknown.

## Picket Fence Spectra



We obtain median picket fence and background spectra (Fig. 3a). The background-subtracted picket fence spectrum (Fig. 3b) reveals prominent GL and  $N_2 1P$  emissions, but no  $N_2^+ 1N$ . Kinetic modeling will evaluate whether a parallel electric field can replicate the observed  $N_2 1P$  to GL emission ratio (Fig. 3c).

Fig 3: (a) Median picket fence and background spectra.

(b) Median picket fence spectrum after background subtraction. Inset: Portion of  $N_2 1P$  spectrum (642 - 700 nm).

(c)  $N_2 1P$  to GL luminosity ratio.  $N_2 1P$  luminosities are scaled to the entire emission band and atmospheric transmission effects are accounted for [8,9].

## Kinetic Model: Emissions due to Parallel Electric Fields

To model the emissions generated by parallel electric fields, we employ a kinetic model in a realistic atmosphere and ionosphere (Fig. 4). Using the BOLSIG+ software [10], we solve the Boltzmann equation for the electron energy distribution function (EEDF) under the influence of parallel electric fields. We then calculate volume emission rates for GL,  $N_2 1P$ , and  $N_2^+ 1N$ , considering electron impact excitation, quenching, and radiative cascade from higher energy states.

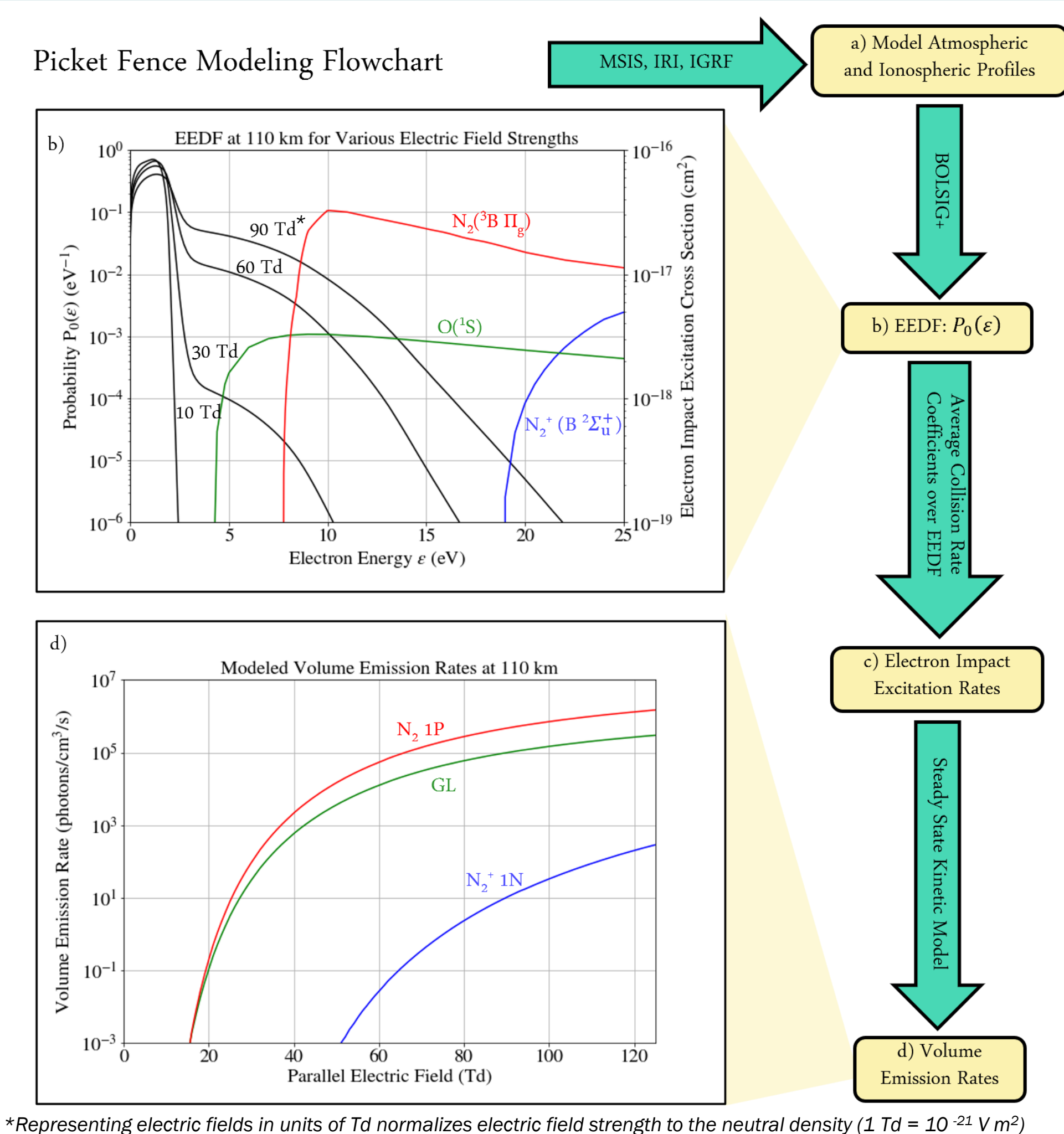
Fig 4: Flowchart of our kinetic modeling process

(a) Initially, we acquire realistic atmospheric and ionospheric profiles for density, temperature, and magnetic field [11,12,13]

(b) Using BOLSIG+ [10], we calculate the EEDF (normalized so  $\int P_0(\epsilon) d\epsilon = 1$ ) with different parallel field strengths. Notably, the EEDF's tail extends as the field strength increases. We overlay relevant electronic excitation cross sections.

(c) To determine electron impact excitation rates, we average the collision rate coefficient (impact excitation collisional cross section times electron velocity) over the EEDF.

(d) Accounting for additional chemical reactions, including quenching and radiative cascade from higher energy states, we obtain volume emission rates that vary with parallel electric field strength.



\*Representing electric fields in units of Td normalizes electric field strength to the neutral density ( $1 \text{ Td} = 10^{-21} \text{ V m}^{-2}$ )

## Results: Data/Model Comparisons

Our modeling results are displayed below (Fig. 5), showing the ratio of the  $N_2 1P$  to GL volume emission rates as a function of electric field strength and altitude. The observed  $N_2 1P$  to GL luminosity ratio and absence of  $N_2^+ 1N$  is replicated for reasonable parallel electric field strengths.

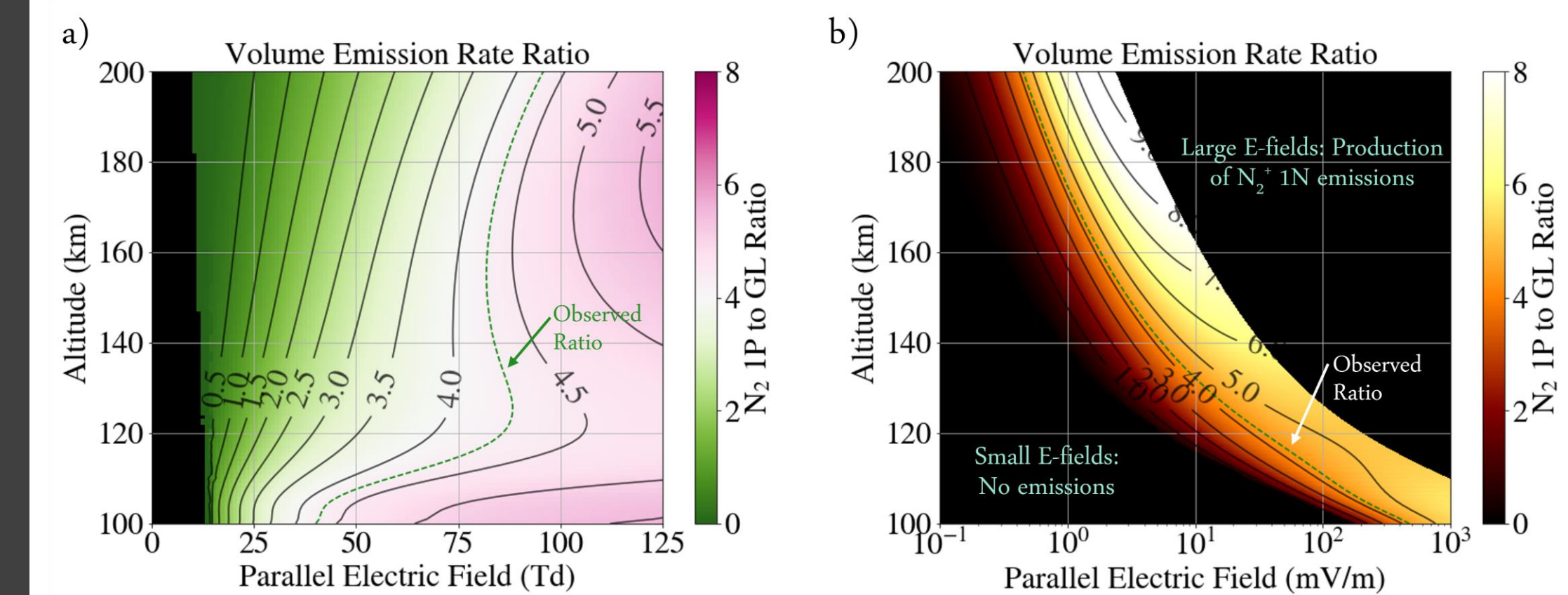


Fig 5: (a) Modeled volume emission ratio between  $N_2 1P$  and GL emissions as a function of altitude and parallel electric field strength measured in Townsend (Td)\*. The observed luminosity ratio (4.28) is highlighted as a green contour line.

(b) The same as (a), but with the electric field expressed in mV/m.

## Discussion and Conclusions

The unique emission spectrum of STEVE's picket fence can be reproduced by a kinetic model driven only by parallel electric fields.

We conclude that magnetospheric particle precipitation is not required for picket fence formation. Our study predicts the electric field strength necessary to replicate the picket fence's spectral features. At a typical picket fence altitude of 110 km [14], we predict electric field strengths of ~60 Td (~100 mV/m). Potential sources of these electric fields will be a topic of future research.

These results are sensitive to atmospheric profiles and transmissivities, which are variable. Future work will evaluate the robustness of these findings when varying these parameters. Further analysis using this model will also predict picket fence spectral features beyond the visible wavelengths.

## Acknowledgements and References

We would like to express our gratitude to Justin Yonker for his valuable assistance in enhancing our understanding of the  $N_2$  triplet cascade. This work was partially supported by NSF grants AGS-1744099 and AGS-2010088 to Penn State University. The TREx data is freely available from <https://data.phys.ucalgary.ca/>.

[1] Nishimura, Y., Dyer, A., Kangas, L., Donovan, E., & Angelopoulos, V. (2023). Unsolved problems in Strong Thermal Emission Velocity Enhancement (STEVE) and the picket fence. *Frontiers in Astronomy and Space Sciences*, 10, 1087974.  
 [2] Nishimura, Y., Gallardo-Lacort, B., Zou, Y., Mishin, E., Knudsen, D. J., Donovan, E. F., ... & Raybell, R. (2019). Magnetospheric signatures of STEVE: Implications for the magnetospheric energy source and interhemispheric conjugacy. *Geophysical Research Letters*, 46(11), 5637-5644.  
 [3] Bennett, C. L., & Bourassa, N. (2021). Improved analysis of STEVE photographs. *Journal of Geophysical Research: Space Physics*, 126(4), e2020JA027843.  
 [4] Mende, S. B., Harding, B. J., & Turner, C. (2019). Subauroral green STEVE arcs: Evidence for low-energy excitation. *Geophysical Research Letters*, 46(24), 14256-14262.  
 [5] Lynch, K. A., McManus, E., Gutov, J., Burlidge, M., & Zettergren, M. (2022). An ionospheric conductance gradient driver for subauroral picket fence visible signatures near STEVE events. *Journal of Geophysical Research: Space Physics*, 127(12), e2022JA030863.  
 [6] Mishin, E. V., & Streitsov, A. V. (2022, December). The Kinetic Theory of STEVE and Picket Fence. In *AGU Fall Meeting Abstracts* (Vol. 2022, pp. SM25E-2016).  
 [7] Gillies, D. M., Donovan, E., Hampton, D., Liang, J., Connors, M., Nishimura, Y., ... & Spanswick, E. (2019). First observations from the TREx spectrograph: The optical spectrum of STEVE and the picket fence phenomena. *Geophysical Research Letters*, 46(13), 7207-7213.  
 [8] Jones, A. V. (2012). *Aurora* (Vol. 9). Page 132. Springer Science & Business Media.  
 [9] Morrill, J. S., Bucsela, E. J., Pasko, V. P., Berg, S. L., Heavner, M. J., Moudry, D. R., ... & Sentman, D. D. (1998). Time resolved  $N_2$  triplet state vibrational populations and emissions associated with red sprites. *Journal of Atmospheric and Solar-Terrestrial Physics*, 60(7-9), 811-829.  
 [10] Hagelaar, G. J. M., & Pitchford, L. C. (2005). Solving the Boltzmann equation to obtain electron transport coefficients and rate coefficients for fluid models. *Plasma sources science and technology*, 14(4), 722.  
 [11] Wardinski, I., Saturnino, D., Amit, H., Chambodut, A., Langlais, B., Manda, M., & Thebaud, E. (2020). Geomagnetic core field models and secular variation forecasts for the 13th International Geomagnetic Reference Field (IGRF-13). *Earth, Planets and Space*, 72(1), 1-22.  
 [12] Picone, J. M., Hedin, A. E., Drob, D. P., & Aikin, A. C. (2002). NRLMSISE-00 empirical model of the atmosphere: Statistical comparisons and scientific issues. *Journal of Geophysical Research: Space Physics*, 107(A12), SIA-15.  
 [13] Bilitza, D., Altavilla, D., Truhik, V., Shubin, V., Galkin, I., Reinsch, B., & Huang, X. (2017). *International Reference Ionosphere 2016: From ionospheric climate to real-time weather predictions*. *Space weather*, 15(2), 418-429.  
 [14] Archer, W. E., St. Maurice, J. P., Gallardo-Lacort, B., Perry, G. W., Cully, C. M., Donovan, E., ... & Euring, D. (2019). The vertical distribution of the optical emissions of a STEVE and Picket Fence event. *Geophysical Research Letters*, 46(19), 10719-10725.